Optical Partial Discharge Detection in Insulating Substrates

Ivan Semenov*, Ingrid Gunheim Folkestad*, Kaveh Niayesh*, Dag Linhjell+, Lars Lundgaard+
* NTNU, Trondheim, 7034, Norway
+ SINTEF Energy, Trondheim, 7034, Norway

Abstract

Photomultiplier tubes (PMT) in combination with flexible liquid light guides and lenses have been tested for partial discharge (PD) detection. The coincidence technique was used to eliminate the random noise of PMTs. Results of PD measurements in two different insulation systems, namely a needle-plane arrangement in air and a ceramic substrate in silicone liquid, are presented and discussed.

1. Introduction

Analysis of phase-resolved patterns of electrical PD pulses can be complicated and insufficient for identifying defects leading to partial discharges [1]. For insulation systems allowing the visual observation of PDs, combining electrical and optical detectors can be a significant help in localizing the PD sites. By using photomultiplier tubes (Fig. 1) sensitive to low energy lights in UV to visible wavelength range, one can measure single PD events or record both electrical and optical phase-resolved patterns with pulse counting instruments [2, 3].

This work demonstrates the use of PMTs with light guides and focusing lenses on PD tests in a needle-plane arrangement in air and ceramic substrates immersed in silicone liquid. The latter has been tested to assess the sensitivity of the optical setup to small external discharges under liquid.

1.1. Photomultiplier

A photomultiplier tube is a vacuum tube made of glass with a photocathode at the front, a row of electron multiplying dynodes, and an anode (Fig. 1). The PMT converts photons hitting the photocathode into electrons and multiplies them through secondary emissions from dynodes into a measurable current signal at the anode. The dynodes are connected to a high supply voltage divided with a resistive voltage divider. The gain of the PMT changes as a power function of the supply voltage. The time interval between the arrival of a photon at the cathode and the start of the current at the anode is called transit time. The transit time is usually in the order of tens of ns and can vary depending on where the photons hit the photocathode.

Even in complete darkness, a PMT generates a small number of current pulses called dark current. The high-rate dark current can reduce the sensitivity of the PMT. The main factors influencing the amount of dark current are ohmic leakage current, thermionic emission, and field effect [4]. The leakage current between the electrodes is critical at lower temperatures or low operating voltages. The thermionic emission from the cathode increases as a power function of temperature. Both the rate and magnitude of dark current increase with temperature. To limit the thermionic dark current the PMTs are usually cooled to 0 to –30°C. The field emission can occur due to local high electric fields in the PMT.

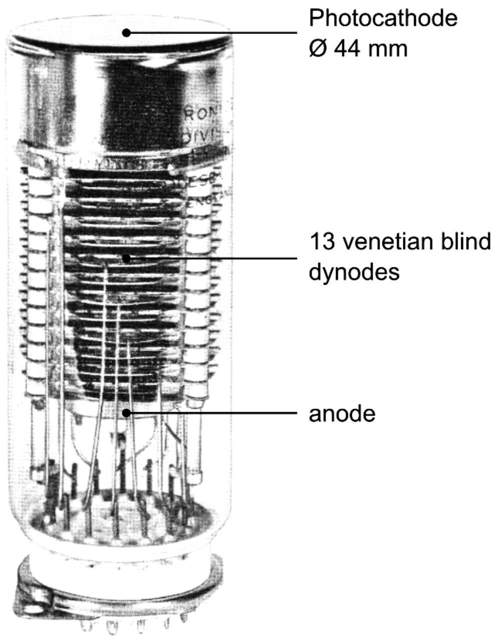

Fig. 1 – Main elements of a photomultiplier tube based on model 6255 EMI [4].

Experiments with PMTs are carried out in dark shielded cabinets or chambers to limit the noise due to ambient light. Mechanical shutters are used to avoid exposure of the light-sensitive photocathode during the preparation of experiments. The sensitivity of PMTs strongly depends on the distance of the PMT from the tested object and the view angle. It is often necessary to adjust the position of the PMTs depending on the object under test. In such cases, a flexible light guide with a high transmission rate can be useful. The light guides are made as hoses filled with liquid and sealed with UV transparent windows on both ends. The liquid light guides with a larger aperture transmit more light than silica fiber bundles. The high flexibility of the light guide allows positioning at different angles and distances from the test object. Also, increasing the distance of the PMT from the current leading parts, reduces the influence of magnetic fields.

2. Experimental
2.1. Optical system

The optical system consists of two identical PMTs with fitted light guides and focusing lenses (Fig. 2). The cathode material of PMTs (EMI 6255) is the UV sensitive S-13 Cs_3Sb-O. The cathode diameter is 44 mm. The tubes were used without cooling. The light guides are 1.5 m in length and 5 mm in diameter with the acceptance cone of 50° (Lumatec Series 250). The transmission spectrum of light guides covers the range from 250 to 700 nm with a maximum transmission of 80% between 300 and 500 nm. The ends of the guides at the sample side were fitted in a rounded aluminum shield and grounded (Fig. 2b). The other ends were fitted to lens holders. In order to focus the beam on the center of the photocathode, two 35 mm plano-convex fused silica lenses 1 inch in diameter were placed between the light guide and the PMT (Fig. 2c).

Knowledge of the transit times of PMTs and attenuations in light guides and lenses is important. In optical setups, the transit times are measured using very short light pulses and mirrors [5]. In this work, the transit time is estimated as the delay between the electrical and optical signals measured for corona discharge at a needle tip. The current pulse was measured by connecting the needle through a 50 Ohm coaxial cable to the 50 Ohm input impedance of the oscilloscope Tektronix DPO4104 with the bandwidth of 1 GHz. The output signal of the PMT was measured on the second channel of the oscilloscope with 50 Ohm input impedance. Equally long cables with similar delay times were used for both signals. The attenuation in the light guide and lenses was roughly measured as the ratio between the amplitudes of anode current pulses from a PMT placed above the needle and a PMT with an attached light guide and lenses.

In the first test, the PMT was placed in the HV cabinet at a distance 45 mm above the needle. The light pulses lagged by 45 ns after the current pulses (Fig. 3a). The electrical pulses had rise times of 2 ns and pulse durations of around 120 ns at the base. The optical pulses had rise times of 9 ns and pulse durations of 60 ns at the base. The jitter and amplitude walk of the optical signals were slightly higher than those of the electrical ones.

In the second test the end of the light guide was placed similarly 45 mm above the needle. The amplitude of the light pulses was almost half of that measured in the first test. The optical pulses featured larger jitter and amplitude fluctuations. While the directly measured light pulses contained a tail due to the ionic tail of the corona discharge, the light pulses measured with the light guide were mainly symmetrical. Interestingly, the transit time in the second test was almost 10 ns longer than in the first test.

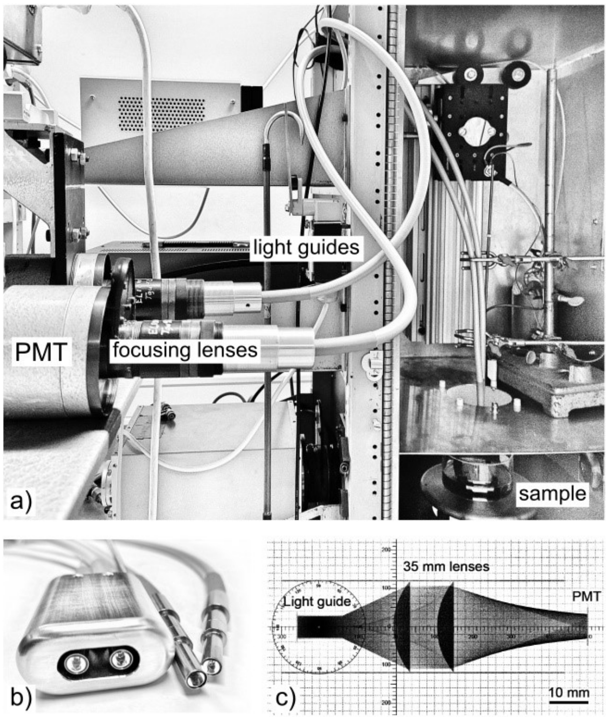

Fig. 2 – Experimental setup for optical PD measurements a) the arrangement of the PMT and light guides, b) liquid light guides mounted in a rounded shield c) the lens construction for focusing the light beam into the PMT.

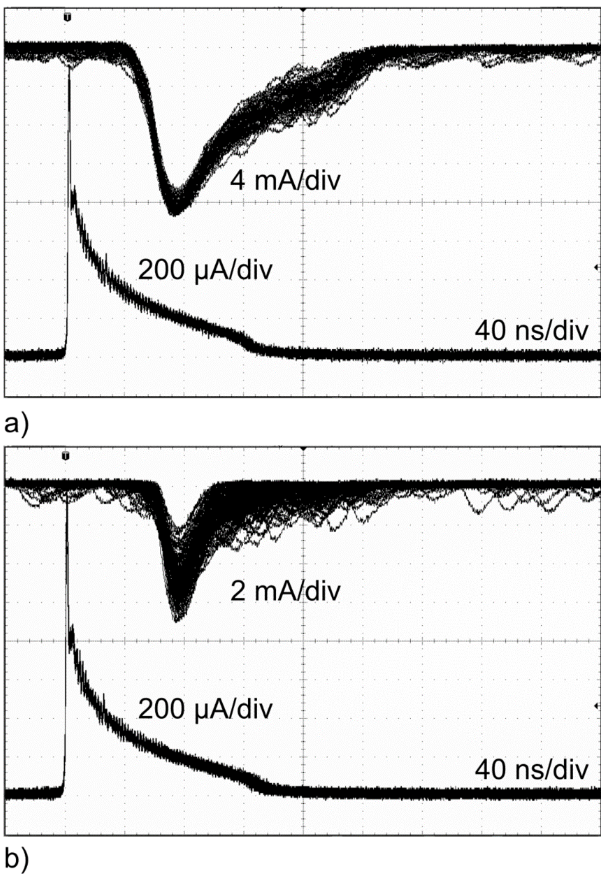

Fig. 3 – Current pulses of negative corona and anode current pulses from the PMT a) the light is measured with the PMT above the sample, b) the light is transmitted into the PMT through a light guide and two fused silica lenses.

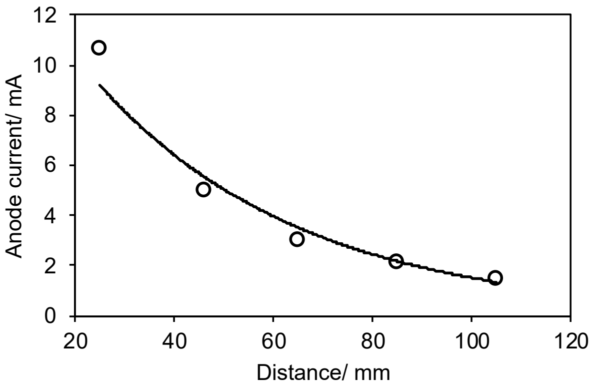

Fig. 4 – Amplitude of the anode current as a function of the distance between the light guide end and the needle tip. The points are fitted with an exponential function.

The attenuation of the light signals increased almost exponentially with the distance between the end of the light guide and the needle (Fig. 4). The distance in HV experiments is defined by the safe clearance distance from the parts under high voltage. In this test, both the needle and the light guide were grounded.

Overall, the PMTs produced considerable amounts of dark current with a repetition rate that makes it hard to detect weak light pulses especially on time base of 20 ms e. g., for power frequency sinusoidal voltage.

2.2. Coincidence technique

The thermal and ambient light noise can be eliminated by using the coincidence technique i.e., by detecting only coinciding signals. This technique is widely used in particle detection experiments. The coincidence circuit used in this work is built of two PMTs and a set of standardized nuclear instrumentation modules (NIM) i.e., amplifiers, a pulse discriminator, a logic unit, a delay amplifier, and a linear gate (Fig. 5). The coincidence circuit produces an analog logic signal once two coinciding light signals are detected. To obtain the information about the intensity of the detected light, the signal from one of the PMTs is amplified with a shaping amplifier.

The outputs of PMTs are connected via 50 Ohm coaxial cables to the identical inputs of a constant fraction discriminator (CFD) [6]. The CFD is a timing discriminator that allows constant fraction timing for fast pulses arriving directly from PMTs. The signal threshold and the constant fraction setting can be adjusted according to the noise level and the pulse rate of input signals. The CFD generates a NIM standard fast negative logic pulse i.e., –14...–18 mA into a 50 Ohm impedance. The advantage of the constant fraction discriminator is that no additional timing delay is introduced depending on the amplitude of the input signal as in case of single-channel analyzers with edge timing. The width of the output signals of the CFD was set to 200 ns.

The outputs of the CFD are connected to the identical inputs of a logic unit performing the function of a coincidence i.e., AND-logic. The two NIM input signals

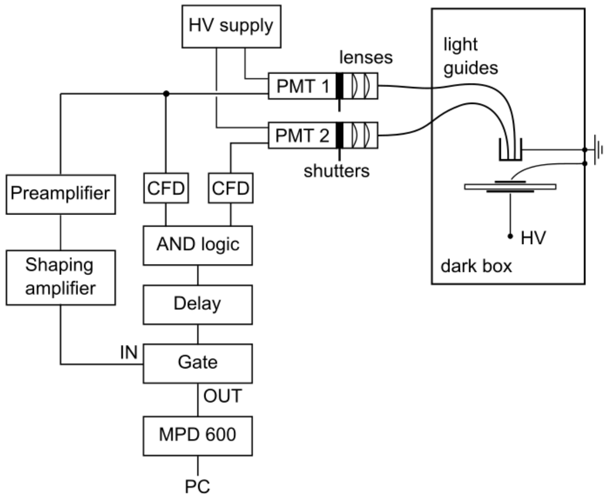

Fig. 5 – Setup for optical PD measurements at sinusoidal voltage. The coincidence circuit built of NIM components:

- Tennelec T145 preamplifier
- Tennelec TC241 shaping amplifier
- Ortec Quad 935 constant fraction discriminator
- Ortec CO4020 Quad 4-input logic unit
- Tennelec TC 308 dual linear gate.

must be in coincidence i.e., overlap by at least 3 ns for the logic unit to generate a fast NIM and TTL signals on the output. The width of the output signal was set to 240 ns (cf. signal 2 in Fig. 6).

The output of the logic unit controls the linear gate. The linear gate lets through a part of the amplified light signal that passes through a charge-sensitive preamplifier and a shaping amplifier (Fig. 5). This path causes a delay of around 350 ns (cf. signals 1 and 3 excluding the PMT transit time 50 ns in Fig. 6). The shaping amplifier generated a bipolar pulse with a peaking time of 640 ns. The gate control signal was delayed by 750 ns with a delay amplifier to match it to the peak of the shaped pulse. Herewith, a fraction of the amplified signal that carries the information of the peak amplitude passes

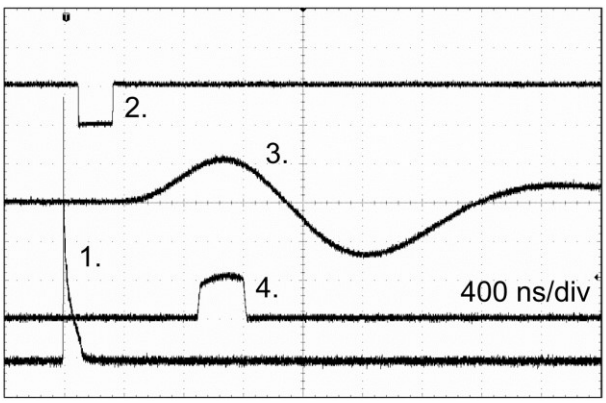

Fig. 6 – Oscillographs of 1) corona discharge current, 200 µA/div, 2) logic unit output, 1 V/div, 3) output of the shaping amplifier with gain 500, 2V/div, 4) fraction of the amplified signal passing through the linear gate 2V/div. The gate control signal is delayed by 750 ns.

through the linear gate. In this work, the output of the coincidence circuit was connected to the PD input of the Omicron MPD 600 partial discharge detection unit. The gain of the shaping amplifier and the MPD 600 were adjusted according to the intensity of light emitted from the measured discharges. Fig. 6 shows the corona discharge pulse and the signals from single components of the coincidence circuit. The resulting delay between the electrical and optical signals counts approximately 880 ns.

3. Testing measuring principle

3.1. Needle-plane

To test the measuring principle, the electrical and optical PD signals were recorded as phase-resolved PD patterns (PRPD). Two synchronized PD detection instruments MPD 600 were used to record and integrate the electrical and optical signals. The electrical current pulses were measured with a PD measurement impedance Omicron CPL 542 and integrated with the center frequency 250 kHz and a bandwidth of 300 kHz according to IEC 60270. The second MPD600 unit integrated the optical signal i.e., the output of the coincidence circuit proportional to the light intensity (signal 4 in Fig. 6). The amplitude of light signals is arbitrary since it depends on the gain of the shaping amplifier and the signal width selected according to the object under test.

In the first test, a single PMT was placed above the needle. To record all light signals above the noise level,

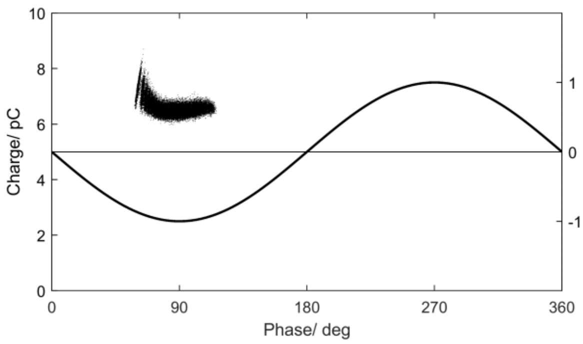

a)

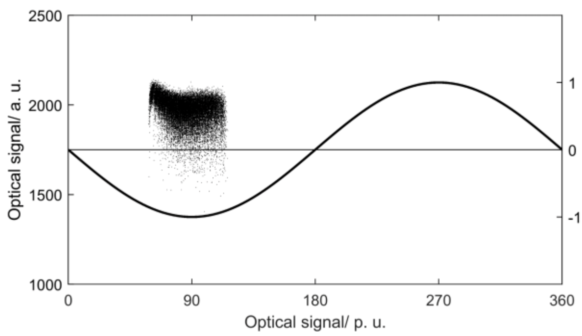

b)

Fig. 9 – PRPD patterns for negative corona discharge. Pulse counts a) electrical signals, 37572 pulses, b) optical signals, 37572 pulses in 46 seconds.

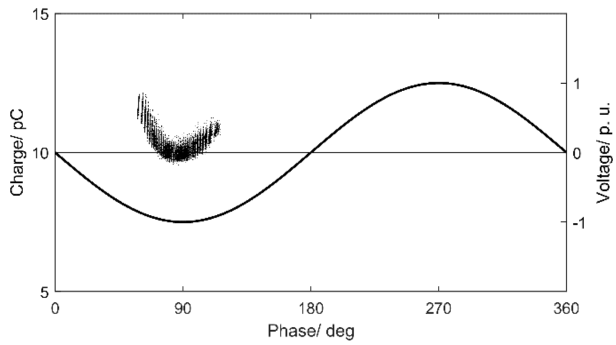

a)

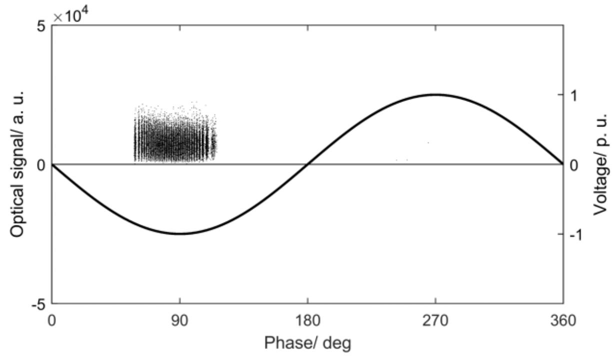

b)

Fig. 10 – PRPD patterns for negative corona discharge. Pulse counts a) electrical signals, 23586 pulses, b) optical signals, 23258 pulses in 22 seconds.

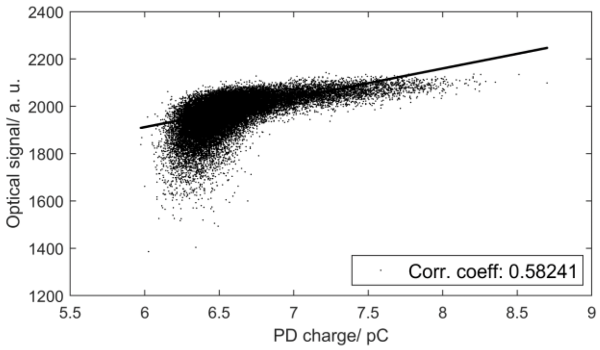

a)

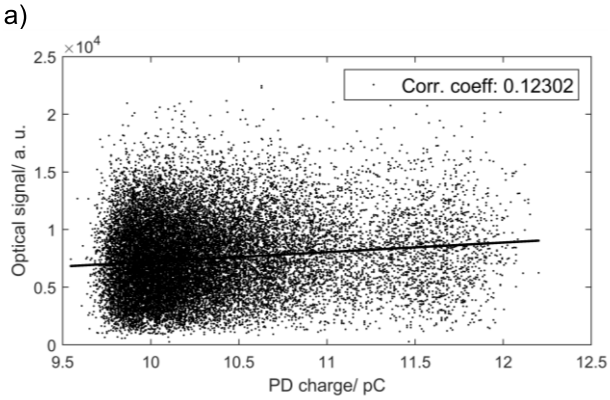

b)

Fig. 11 – Amplitude correlation of electrical and optical pulses optical signals were measured a) with a PMT above the needle, b) with light guides and lenses.

the logic unit of the coincidence circuit was deactivated, and the threshold of the constant fraction discriminator was set above the noise level. As the patterns show, the number of recorded electrical and optical signals was identical and distributed in a similar way (Fig. 9). The delay between optical and electrical pulses of around 900 ns was insignificant in low-frequency ac measurements. Fig. 11a shows the amplitude correlation between the emitted light and the apparent charge of PDs measured at the same time. The correlation increased towards higher amplitudes of discharges

The optical signals in Fig. 10 were measured using the light guides connected to two PMTs, and the coincidence circuit. Although the number of electrical and optical signals was similar, the amplitude correlation was relatively low (Fig. 11b). This is due to stronger amplitude fluctuations of light signals transmitted through the light guides.

3.2. Ceramic substrate in silicone liquid

One of the purposes of the developed setup is to detect light emitted by PDs in the silicone gel from sharp etched edges at the bonded copper in ceramic substrates (Fig. 12). The optical detection has a significant advantage over the electrical current measurement in experiments where substrates are stressed with fast transient voltages. Due to the high frequency components of such applied voltages, it is impossible to use electrical PD detectors with the bandwidth narrower than 1 MHz. The high charging current makes it difficult to extract the small PD currents.

At sinusoidal voltage, the PD signals were measured with the setup shown in Figs. 2a and 5. Electrical and optical signals were recorded and integrated with two identical PD measurement units MPD600 as described in Section 3.1. The aluminum nitride sample was soldered onto a wider copper plate to reduce the probability of PD inception on the lower invisible side of the substrate (Fig. 12, 13). The sample was covered with silicone liquid under vacuum. The high voltage was applied to the copper base. The upper conductor was connected to ground. The liquid light guides were placed 35mm above the substrate (Fig. 13).

The PD patterns were accumulated for 15 minutes while the voltage was kept constant at 12 kV_p (Fig. 14). The electrical PDs show stronger discharges in the negative polarity but a higher occurrence rate of smaller pulses in the positive polarity. The optical PD pattern approximately reproduces the amplitude and phase distribution of electrical pulses. Some PDs in both half-cycles occur close to voltage zero crossings. Such discharges are incepted under the influence of the electric field induced by the space charge. The discharges are associated with measurable light.

Compared to discharges at the needle tip, in case of the substrate in liquid, much fewer optical pulses were detected. This could be an indication that some PDs occurred inside the ceramic. However, visible PDs of low amplitude could not have been detected due to the light absorption in the liquid. The other reason for the reduced

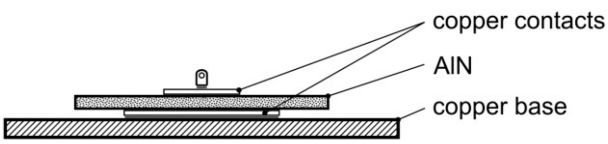

Fig. 12 – Schematic of the AlN substrate soldered onto a copper base.

Fig. 13 – Liquid light guides positioned above the ceramic substrate in silicone liquid to detect visible PDs. The HV electrode is on the bottom of the sample holder.

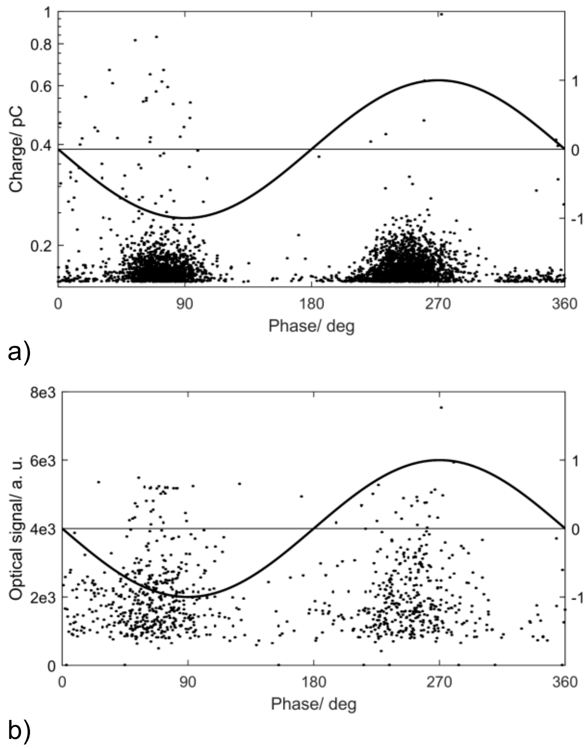

Fig. 14 – PRPD patterns recorded for 15 min on aluminum nitride substrate a) electrical signals 3775 pulses, b) optical signals 939 pulses.

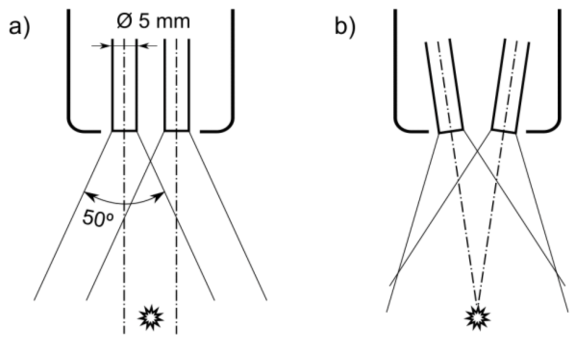

Fig. 15 – Positioning of light guide ends inside the metallic shield.

rate of light detection could be the alignment of the light guides. The light guides were fitted inside the aluminum shield parallel to each other with not fully overlapping view fields as shown in Fig. 15a. With such alignment, the PD sites outside the view field of one of the light guides cannot detected by the coincidence technique. The view fields should be overlapped by positioning the light guides as shown in Fig. 15b to detect all coinciding lights emitted by PDs.

With the optical system consisting of light guides and the coincidence circuit, edge discharges in a ceramic substrate under liquid could be detected. However, it was found that PDs under fast transient voltages could be measured more accurately with a single PMT placed directly above the sample. A high degree of detectivity could be achieved even without the coincidence technique thanks to the much shorter time base in the order of several μs. The setup used for square wave experiments is described in [1]. Fig. 16 shows an envelope of optical signals accumulated over 50 voltage pulses. Almost no dark current noise was recorded before the leading edge of the unipolar negative voltage pulse. For voltage pulses with shorter rise times in the order of 100 ns the delay between the voltage pulse and optical signals should be determined carefully. With corrected signal delays, the instantaneous PD inception voltage levels at the rising or falling edges can be determined.

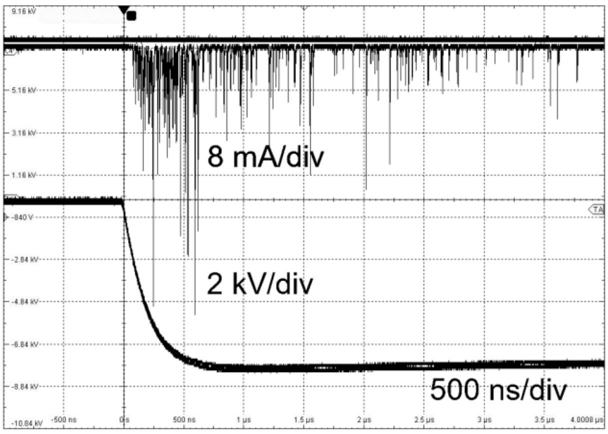

Fig. 16 – Envelopes of light signals accumulated over 50 pulses at 30 Hz at the leading edge of the unipolar negative voltage pulse.

4. Conclusion

The work demonstrates the application of photomultiplier tubes in the optical PD detection for two different objects. The performance of liquid light guides together with focusing lenses was tested. The function of the coincidence technique was explained.

Liquid light guides are suitable for PD tests in which the discharges emit both strong and weak lights e.g., corona discharge in air or small surface discharges under liquid. It is also able to detect sharp edge discharges in substrates under liquid with apparent charges less than 1 pC. However, the light guides considerably attenuate the light and increase the jitter and amplitude walk of optical signals. In the presented example, the attenuation counted almost 50 % for a corona discharge at a needle tip. To improve the sensitivity, a collecting lens could be placed at the sample end of the light guide. The angled positioning of light guides would overlap the fields of view and thus improve the sensitivity. A single bi-convex focusing lens could be used to reduce the light absorption in lenses.

In experiments with fast transient voltages, satisfactory results were obtained with a single PMT used without a light guide. The setup proved to be sensitive to small edge discharges observed in a ceramic substrate immersed into silicone liquid. Measuring the PD inception voltages by using the same PMT at sinusoidal and square voltage waveshapes can provide a base for studies of effects related to voltage waveshapes.

5. Acknowledgments

These results were produced in the FastTrans project funded by the Norwegian Research Council under contract 294508, and supported by ABB AS, Infineon, Total E&P Norge AS, Aker BP ASA, Equinor AS, Statnett SF, Statkraft SF and Elvia AS.

6. References

[1] I. Semenov, I. G. Folkestad, K. Niayesh, H. K. H. Meyer and L. Lundgaard, "Investigation of Partial Discharges in AlN Substrates under Fast Transient Voltages," IEEE Transactions on Dielectrics and Electrical Insulation, 2022.

[2] H. Raether, Electron Avalanches and Breakdown in Gases. Butterworths, 1964.

[3] L. E. Lundgaard and S. L. Kyrkjeeide, "Evaluation of dielectric liquids by measurement of their partial discharge characteristics," Proceedings of IEEE Conference on Electrical Insulation and Dielectric Phenomena - (CEIDP'94), 1994.

[4] EMI Photomultiplier tubes. EMI Electronics. 1970.

[5] T. Richards, J. Peatross, M. Ware, L. Rees, "Electron transit time measurements of 5-in photomultiplier tubes", Nuclear Instruments and Methods in Physics Research Section A: Accelerators, Spectrometers, Detectors and Associated Equipment, Volume 828, 2016.

[6] Model 935 Quad Constant Fraction 200 MHz Discriminator Operating and Service Manual. ORTEC, 2003.